Supporting Information

Exploring a new synthesis route to lithium-excess disordered rock salt (DRX) cathode materials

Matthew S. Chambers[a]*, Tianyu Li[b], Zhilin Liang[c], Jong Keum[d,e], Kevin H Stone[c], Raphaële J. Clément[b], Beth L. Armstrong[f]*, Ethan C. Self[a]*

[a] Chemical Sciences Division, Oak Ridge National Laboratory, Oak Ridge, TN 37831, USA

[b] Materials Department and Materials Research Laboratory, University of California Santa Barbara, Santa Barbara, CA 93106, USA

[c] Stanford Synchrotron Radiation Lightsource, SLAC National Accelerator Laboratory, Menlo Park, CA 94025, USA

[d] Center for Nanophase Materials Sciences, Oak Ridge National Laboratory, Oak Ridge, TN 37831, USA

[e] Neutron Scattering Division, Oak Ridge National Laboratory, Oak Ridge, TN 37831, USA

[f] Materials Science and Technology Division, Oak Ridge National Laboratory, Oak Ridge, TN 37831, USA.

*Corresponding author

Starting models used in Rietveld refinements

Table S1 – The starting models used in Rietveld refinements throughout this study.

Compound	Reference
$Li_{1.2}Mn_{0.4}Ti_{0.4}O_2$ ⑤	Moghadam *et al.*[1]
$Li_{1.1}Mn_{0.8}Ti_{0.1}O_2$ ⑤	Moghadam *et al.*[1]
Li_2TiO_3	Mukai *et al.*[2]
Li_2MnO_3	Boulineau *et al.*[3]
$LiMn_2O_4$	Berg *et al.*[4]
$LiMnO_2$	Croguennec *et al.*[5]
LiF	Streltsov *et al.*[6]
$LiNO_3$	Wu *et al.*[7]
Mn_2O_3	Geller[8]
Li_2MnO_2	David *et al.*[9]

⑤Structure edited to match stoichiometry, but cell parameters adopted from reference.

Structural analysis of oxide precursors

Figure S1 shows powder X-ray diffraction (XRD) patterns obtained on the $Li_{1.2}Mn_{0.5}Ti_{0.1}O_{1.95}$ and $Li_{1.2}Mn_{0.7}Ti_{0.1}O_{1.85}$ precursors produced *via* the combustion reaction. Both precursors contain multiple crystalline phases including Mn_2O_3 and unreacted $LiNO_3$. The $Li_{1.2}Mn_{0.5}Ti_{0.3}O_{1.95}$ sample also contains $LiMn_2O_4$. Because the $LiNO_3$ has much sharper Bragg peaks than the Mn_2O_3 and $LiMn_2O_4$ phases, two separate peak shapes were used (all Thompson-Hastings-Cox pseudo-Voigt functions). Notably, good fits are obtained in both patterns without including any Ti-containing phases, but ICP-OES (Table S3) indicates that Ti is present in the precursors as expected. This suggests that Ti^{4+} is likely doped into one or more crystalline phases (*e.g.*, $Mn_{2-x}Ti_xO_{3+\delta}$ or $LiMn_{2-x}Ti_xO_{4+\delta}$) or present as an amorphous phase. Due to the similar X-ray form factors of Ti^{4+}, Mn^{3+}, and Mn^{4+}, the present dataset cannot distinguish the distribution of Mn and Ti across these phases. The presence of unreacted $LiNO_3$ indicates the combustion reactions did not go to stoichiometric completion. Furthermore, the presence of $LiNO_3$ explains the hygroscopic nature of the precursors as mentioned in the experimental procedures.

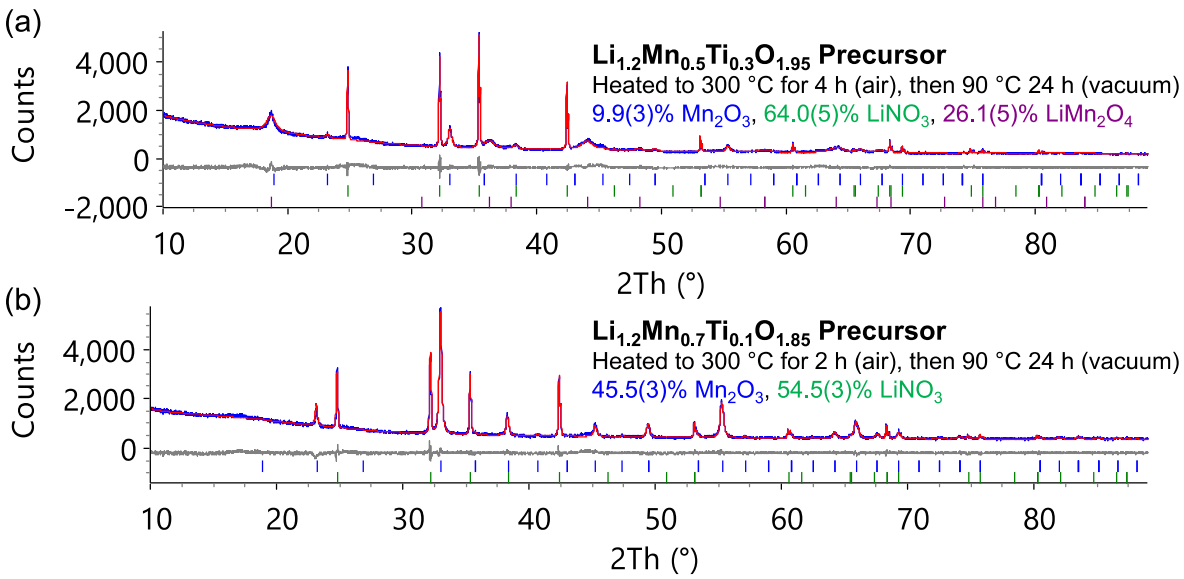

Figure S1 – Rietveld plots (Cu radiation) of precursors produced from combustion reactions including: (a) $Li_{1.2}Mn_{0.5}Ti_{0.3}O_{1.95}$ and (b) $Li_{1.2}Mn_{0.7}Ti_{0.1}O_{1.85}$. Blue curves = observed data; red curves = calculated pattern; grey curves = difference between observed and calculated patterns. Tick marks correspond to reflections arising from each phase.

Summary of the reaction conditions investigated in this study

Table S2 – Summary of synthesis conditions explored in this study. The phase composition of each product was determined through Rietveld refinements which are shown in the corresponding figures. All high-temperature reactions were performed under flowing Ar.

Reactants	Reaction Conditions	Product Composition	Corresponding Figure
$Li_{1.2}Mn_{0.5}Ti_{0.3}O_{1.95}$	1000 °C, 4 h	47.6(8)% DRX 45.9(8)% m-Rock Salt 6.5(5)% $LiMn_2O_4$	Figure 1a
$Li_{1.2}Mn_{0.5}Ti_{0.3}O_{1.95}$ + 0.025Li_2O (Ground in Air)	1000 °C, 1 h	53.1(7)% DRX 42.6(7)% m-Rock Salt 4.3(3)% $LiMn_2O_4$	Figure 1b
$Li_{1.2}Mn_{0.5}Ti_{0.3}O_{1.95}$ + 0.05LiF (Ground in Air)	1000 °C, 1 h	94.1(2)% DRX 3.25(18)% m-Rock Salt 2.70(13)% $LiMn_2O_4$	Figure 2a
$Li_{1.2}Mn_{0.5}Ti_{0.3}O_{1.95}$ + 0.05LiF (Ground in Air)	800 °C, 1 h	86.4(3)% DRX 12.1(6)% m-Rock Salt 1.56(16)% o-Rock Salt	Figure 2b
$Li_{1.2}Mn_{0.5}Ti_{0.3}O_{1.95}$ + 0.05LiF (Ground in Air)	1000 °C, 4 h	69.3(4)% DRX 30.7(4)% m-Rock Salt	Figure S2a
$Li_{1.2}Mn_{0.5}Ti_{0.3}O_{1.95}$ + 0.05LiF (Ground under Ar)	800 °C, 1 h	92.0(2)% DRX 8.0(2)% m-Rock Salt	Figure S2b
$Li_{1.2}Mn_{0.7}Ti_{0.1}O_{1.85}$	1000 °C, 1 h	0.8(2)% $LiMn_2O_4$ 66.6(5)% m-Rock Salt 28.0(5)% o-Rock Salt 4.6(4)% Li_2MnO_2	Figure 6a
$Li_{1.2}Mn_{0.7}Ti_{0.1}O_{1.85}$ + 0.15LiF (Ground in Air)	1000 °C, 1 h	81.5(8)% DRX 11.8(3)% m-Rock Salt 7.2(9)% LiF	Figure 6b
$Li_{1.2}Mn_{0.7}Ti_{0.1}O_{1.85}$ + 0.15LiF (Ground under Ar)	1000 °C, 1 h	78(4)% DRX 8.1(5)% m-Rock Salt 14(4)% LiF	Figure S2c
$Li_{1.2}Mn_{0.7}Ti_{0.1}O_{1.85}$ + 0.15LiF (Ground under Ar)	800 °C, 1 h	12.6(7)% DRX 33.3(11)% m-Rock Salt 9.5(4)% o-Rock Salt 11.6(6)% $LiMn_2O_4$ 33(2)% LiF	Figure S2d

Additional Rietveld plots

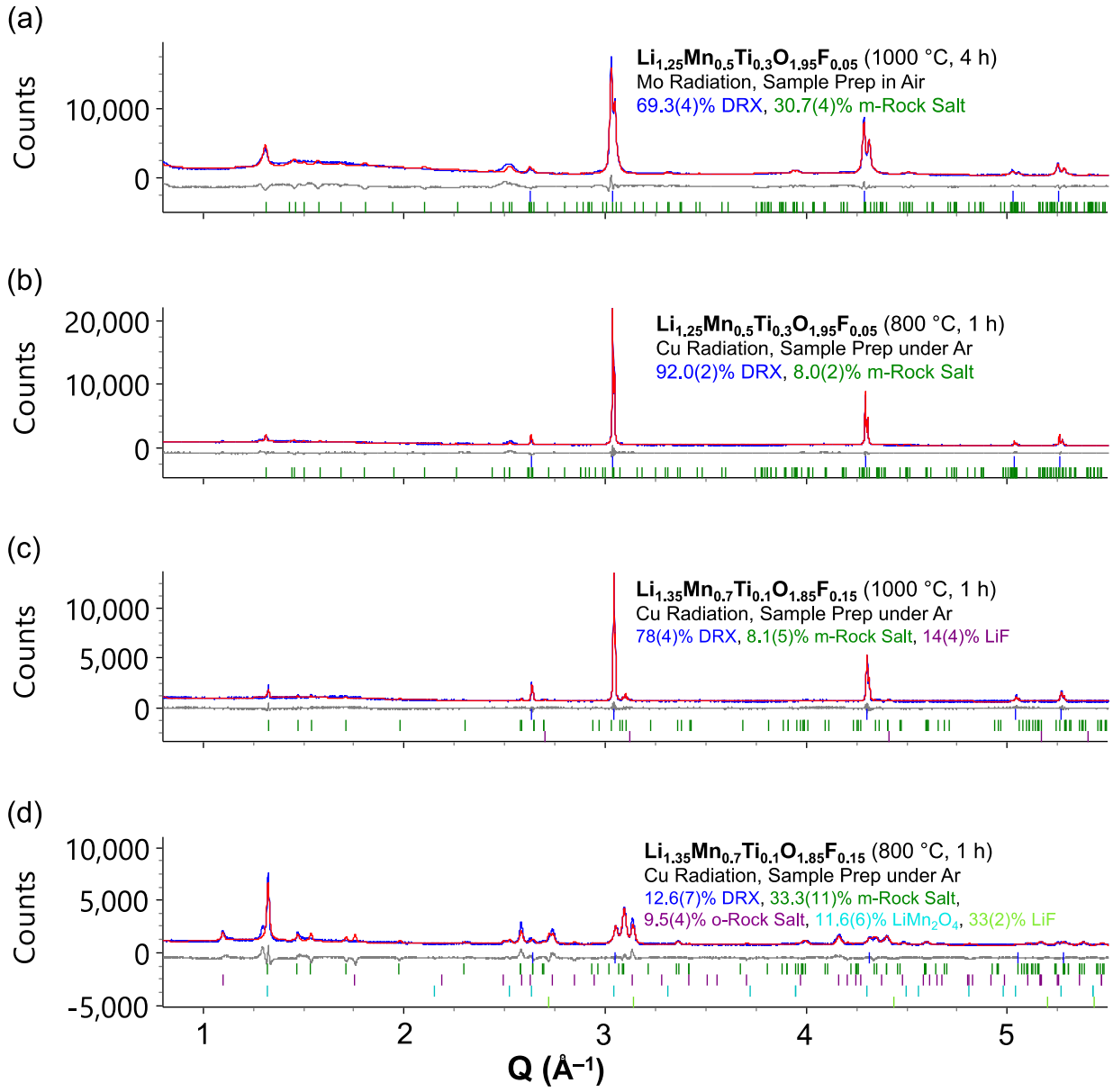

Figure S2 – Additional Rietveld plots for oxyfluoride products obtained by reacting the oxide precursor with LiF. These plots include (a) $Li_{1.25}Mn_{0.5}Ti_{0.3}O_{1.95}F_{0.05}$ (reagents ground in air), R_{wp} = 9.967%, χ^2 = 2.883, (b) $Li_{1.25}Mn_{0.5}Ti_{0.3}O_{1.95}F_{0.05}$ (dried reagents ground under Ar), R_{wp} = 6.677%, χ^2 = 1.795, (c) $Li_{1.35}Mn_{0.7}Ti_{0.1}O_{1.85}F_{0.15}$ (dried reagents ground under Ar), R_{wp} = 4.557%, χ^2 = 1.365, and (d) $Li_{1.35}Mn_{0.7}Ti_{0.1}O_{1.85}F_{0.15}$ (dried reagents ground under Ar), R_{wp} = 8.000%, χ^2 = 2.647. Blue curves = observed data; red curves = calculated data; grey curves = difference between observed and calculated patterns. Tick marks correspond to reflections arising from the corresponding phase.

^{19}F ssNMR fits using longer relaxation times (D1 = 20 s)

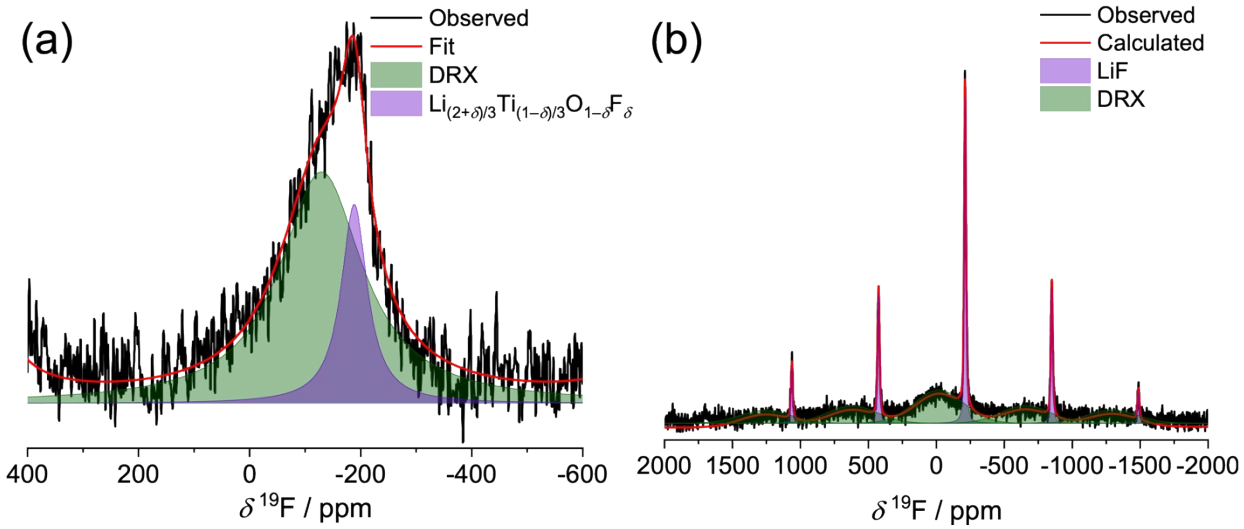

Figure S3 – Fits against ^{19}F NMR data with a lifetime of D1 = 20s for (a) $Li_{1.25}Mn_{0.5}Ti_{0.3}O_{1.95}F_{0.05}$ heated at 800 °C for 1h and (b) $Li_{1.35}Mn_{0.7}Ti_{0.1}O_{1.85}F_{0.15}$ heated at 1000 °C for 1 h.

Characterization of Li_3TiO_3F

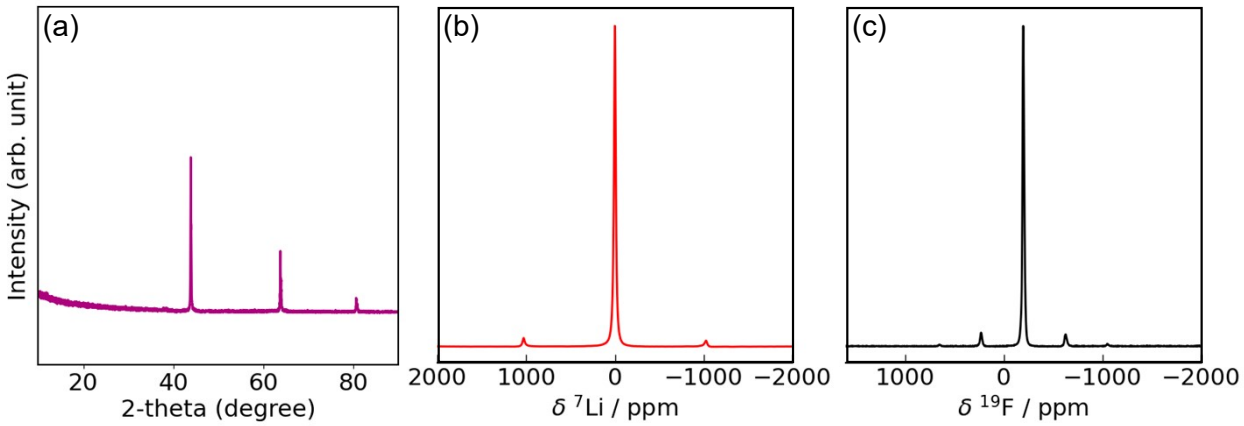

Figure S4 – Characterization of Li_3TiO_3F including (a) XRD pattern (Cu radiation), (b) ^{7}Li ssNMR spectrum, and (c) ^{19}F ssNMR spectrum.

Additional SEM images

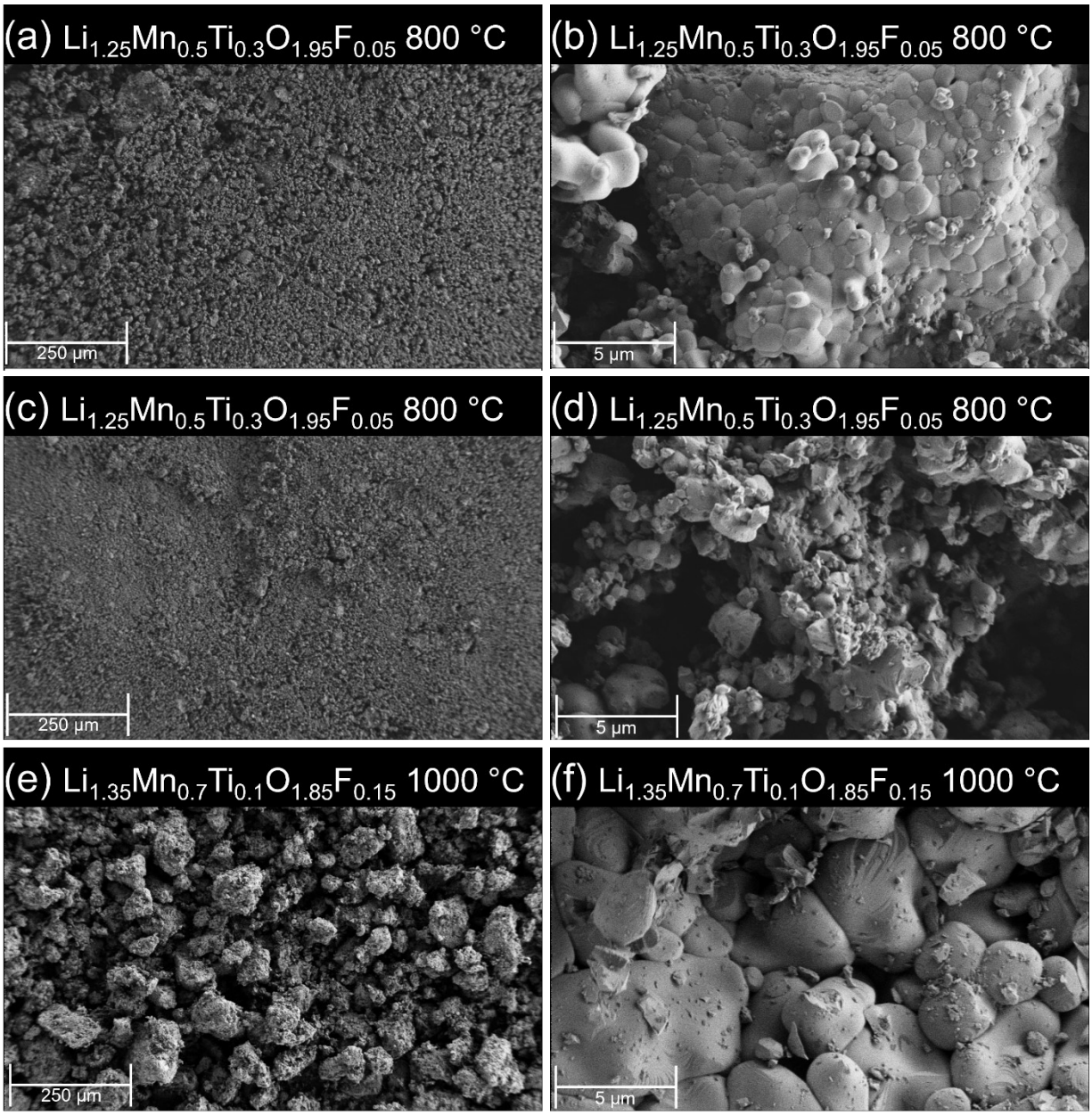

Figure S5 – SEM images of select samples including: (a)–(b) $Li_{1.25}Mn_{0.5}Ti_{0.3}O_{1.95}F_{0.05}$ heated at 800 °C for 1 h (reagents ground in air), (c)–(d) $Li_{1.25}Mn_{0.5}Ti_{0.3}O_{1.95}F_{0.05}$ heated at 800 °C for 1 h (dried reagents ground under Ar), and (e)–(f) $Li_{1.35}Mn_{0.7}Ti_{0.1}O_{1.85}F_{0.15}$ heated at 1000 °C for 1 h (dried reagents ground under Ar).

Additional electrochemical data

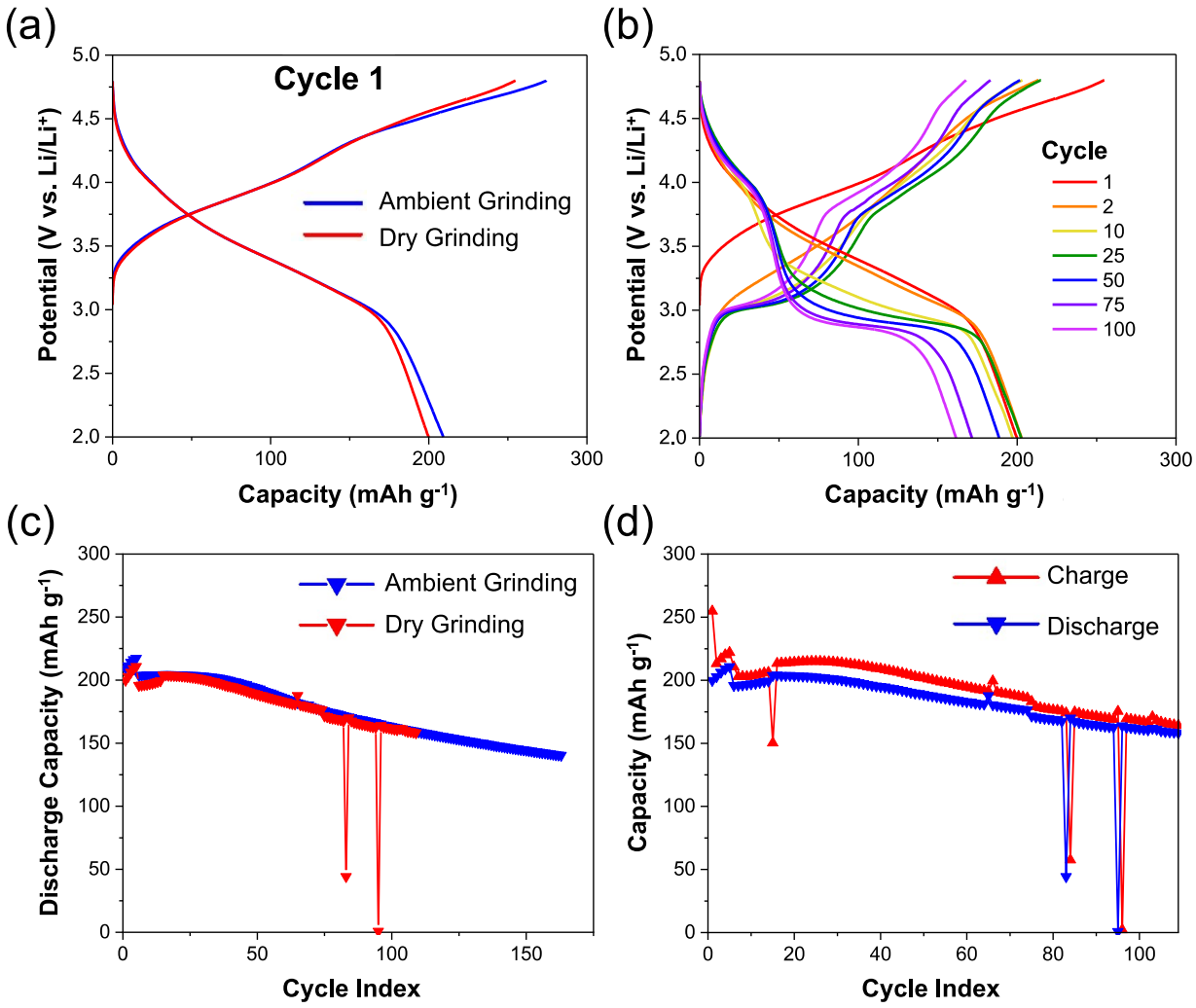

Figure S6 – Galvanostatic cycling performance of $Li_{1.35}Mn_{0.7}Ti_{0.1}O_{1.85}F_{0.15}$ cathodes which were prepared by grinding the oxide precursor with LiF either in air ("Ambient Grinding") or under an Ar atmosphere ("Dry Grinding"). (a) Voltage profiles of the ambient-ground and dry-ground samples during the first cycle, (b) voltage profile of the dry-ground sample during extended cycling, (c) discharge capacity of the ambient-ground and dry-ground samples, and (d) charge/discharge capacity of the dry-ground sample. The anomalous results at cycles 15, 83, 84, 95 and 96 in (c) and (d) are due to power outages.

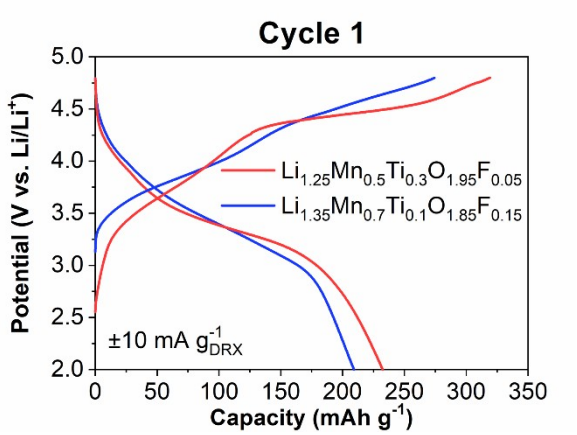

Figure S7 – First cycle voltage profiles for DRX cathodes with nominal compositions of $Li_{1.25}Mn_{0.5}Ti_{0.3}O_{1.95}F_{0.05}$ and $Li_{1.35}Mn_{0.7}Ti_{0.1}O_{1.85}F_{0.15}$. Samples were cycled galvanostatically at a specific current of ±10 mA/g_{DRX}. $Li_{1.25}Mn_{0.5}Ti_{0.3}O_{1.95}F_{0.05}$ and $Li_{1.35}Mn_{0.7}Ti_{0.1}O_{1.85}F_{0.15}$ were synthesized by annealing at 1000°C for 2 h and 1 h, respectively.

Table S3 – Nominal and quantitative compositions (as determined from ICP-OES/F-ISE measurements) of select DRX oxyfluorides. The lower-than-expected Mn/Ti ratio measured for the $Li_{1.25}Mn_{0.5}Ti_{0.3}O_{1.95}F_{0.05}$ powders was due to errors introduced by an aged (*i.e.*, partially evaporated) Ti-based precursor which altered the effective Ti concentration in solution. The $Li_{1.35}Mn_{0.7}Ti_{0.1}O_{1.95}F_{0.15}$ powders were derived from a fresh Ti reagent which was not subject to this error.

Nominal Formula	Annealing Conditions	Quantitative Formula
$Li_{1.25}Mn_{0.5}Ti_{0.3}O_{1.95}F_{0.05}$	1000 °C, 1 h	$Li_{1.23}Mn_{0.36}Ti_{0.40}O_{1.95}F_{0.03}$
$Li_{1.25}Mn_{0.5}Ti_{0.3}O_{1.95}F_{0.05}$	800 °C, 1 h	$Li_{1.25}Mn_{0.36}Ti_{0.41}O_{1.95}F_{0.05}$
$Li_{1.35}Mn_{0.7}Ti_{0.1}O_{1.95}F_{0.15}$	1000 °C, 1 h	$Li_{1.26}Mn_{0.72}Ti_{0.11}O_{1.85}F_{0.15}$

References

1. Y. Shirazi Moghadam, A. El Kharbachi, T. Diemant, G. Melinte, Y. Hu and M. Fichtner, *Chemistry of Materials*, 2021, **33**, 8235-8247.
2. K. Mukai, M. Yashima, K. Hibino and T. Terai, *ACS Applied Energy Materials*, 2019, **2**, 5481-5489.
3. A. Boulineau, L. Croguennec, C. Delmas and F. Weill, *Solid State Ionics*, 2010, **180**, 1652-1659.
4. H. Berg, J. O. Thomas, W. Liu and G. C. Farrington, *Solid State Ionics*, 1998, **112**, 165-168.
5. L. Croguennec, P. Deniard, R. Brec and A. Lecerf, *Journal of Materials Chemistry*, 1995, **5**, 1919-1925.
6. V. A. Streltsov, V. G. Tsirelson, R. P. Ozerov and O. A. Golovanov, *Kristallografiya*, 1988, **33**, 90-97.
7. X. Wu, F. R. Fronczek and L. G. Butler, *Inorganic Chemistry*, 1994, **33**, 1363-1365.
8. S. Geller, *Acta Crystallographica Section B*, 1971, **27**, 821-828.
9. W. I. F. David, J. B. Goodenough and M. Thomas, *REVUE DE CHIMIE MINERALE*, 1983, **20**, 636-642.